Numerical Investigation of Edge Flame Structure of Counterflow Nonpremixed Flames with Local Extinction Due to Flame Stretch*

Susumu NODA** and Tomonori TSUBOKURA***

Laminar counterflow nonpremixed flames with local extinction caused by nonuniform inflows are numerically investigated in two-dimensions in a system governed by Lewis numbers of unity and assuming a single-step, irreversible, finite-rate reaction. A numerical method based on the SIMPLE algorithm is used. Edge flame structures are investigated through the introduction of a new progress variable defined as the normalized integral of the mass fraction of a product in the mixture fraction Z space and which expresses the progress of the chemical reaction. Calculation results reveal that the edge flame structure can be classified into three regions; fully burning flame, weakened flame with a low reaction rate, and a non-reacting preheat region. Under these conditions, and in terms of the energy balance, the edge flame structure is dependent on the Z-directional heat diffusion transport, heat consumption (given by the progress variable), and heat production by chemical reaction. It is found that each type of flame structure can be well characterized by three parameters; the mixture fraction, the stoichiometric scalar dissipation rate, and the progress variable. These three parameters are identified as important factors affecting the edge flame structure of nonpremixed flames with local extinction.

Key Words: Combustion Phenomena, Counterflow Nonpremixed Flame, Edge Flame, Flamelet Model, Progress Variable

1. Introduction

Flames subject to local extinction are frequently observed in turbulent flames, and the partial premixing that occurs as a result is thought to be related to a reduction in NOx emission[1], which is of practical interest for turbulent diffusion flames. Lifted turbulent diffusion flames are also subject to partial premixing and local extinction due to flame stretch, which is related to flame stability. The edge flame structure is considered to be useful for characterizing such phenomena[2]-[4].

The transient flamelet model[5],[6], developed to predict turbulent autoignition phenomena through the introduction of progress variables, is attractive in that the model is possibly extendable to the estimation of local extinction, including the flame base structure of lifted nonpremixed flames. On the other hand, Müller et al.[7], who dealt with the scalar G equation, used the weighted sum of unburned and burned flame properties to express the transient flame structure. This is one model of the edge flame structure, however, the progress variable used in the work of Zhang et al.[5] seems to be more appropriate for expressing the transient flame structure. The introduction of the progress variable is closely related to the triple flame structure studied by Buckmaster and Matalon[8] 1988), Dold[9], Kioni et al.[10], Kioni et al.[11], and Ruetsch et al.[12]; in other words, the progress variable more fully describes premixed flame characteristics.

We are concerned in this paper with the numerical investigation of steady, two-dimensional, laminar counterflow diffusion flames with local extinction in nonuniform inflow fields, as part of our research on the edge flame structure in turbulent diffusion flame modeling. In this paper, an attempt is made to systematically characterize the transient flame structure in this system through the intro-

* Received 14th June, 2005 (No. 05-4075)

** Department of Mechanical Engineering, Toyohashi University of Technology, 1-1 Hibarigaoka, Tempaku, Toyohashi 441-8580, Japan. E-mail: noda@mech.tut.ac.jp

*** Graduate Student, Department of Mechanical Engineering, Toyohashi University of Technology, 1-1 Hibarigaoka, Tempaku, Toyohashi 441-8580, Japan

duction of an additional variable, i.e. a progress variable, to be used in conjunction with the mixture fraction and the scalar dissipation rate. The model is evaluated using numerical data for counterflow nonpremixed flames with local extinction, which occur under nonuniform inflow conditions.

2. Formulation and Numerical Scheme

In this study we consider two-dimensional, locally quenching, laminar, methane/air counterflow nonpremixed flames, neglecting the effects of gravity and restricting variable density effects to within a low Mach number limit. All species are assumed to behave as perfect gases, with mass diffusivity equal to heat diffusivity according to assumed Lewis numbers of unity, and combustion is assumed to occur according to a single-step, irreversible, finite-rate reaction. Radiation, bulk viscosity, body forces, diffusion by the Soret and Dufour effects, and pressure gradient diffusion are also neglected.

The resulting governing equations are written in the following form using the standard notation:

Continuity equation,

$$\frac{\partial \rho}{\partial t}+\frac{\partial}{\partial x}(\rho u)+\frac{\partial}{\partial y}(\rho v)=0 \tag{1}$$

Inflow direction (x) momentum equation,

$$\frac{\partial u}{\partial t}+u\frac{\partial u}{\partial x}+v\frac{\partial u}{\partial y}=\frac{1}{\rho}\left\{-\frac{\partial p}{\partial x}+\frac{\partial}{\partial x}\left[\frac{2}{3}\mu\left(2\frac{\partial u}{\partial x}-\frac{\partial v}{\partial y}\right)\right]+\frac{\partial}{\partial y}\left[\mu\left(\frac{\partial u}{\partial y}+\frac{\partial v}{\partial x}\right)\right]\right\} \tag{2}$$

Outflow direction (y) momentum equation,

$$\frac{\partial v}{\partial t}+u\frac{\partial v}{\partial x}+v\frac{\partial v}{\partial y}=\frac{1}{\rho}\left\{-\frac{\partial p}{\partial y}+\frac{\partial}{\partial x}\left[\mu\left(\frac{\partial u}{\partial y}+\frac{\partial v}{\partial x}\right)\right]+\frac{\partial}{\partial y}\left[\frac{2}{3}\mu\left(-\frac{\partial u}{\partial x}+2\frac{\partial v}{\partial y}\right)\right]\right\} \tag{3}$$

Continuity equation of species i,

$$\frac{\partial Y_i}{\partial t}+u\frac{\partial Y_i}{\partial x}+v\frac{\partial Y_i}{\partial y}=\frac{1}{\rho}\left[\frac{\partial}{\partial x}\left(\rho D_m\frac{\partial Y_i}{\partial x}\right)+\frac{\partial}{\partial y}\left(\rho D_m\frac{\partial Y_i}{\partial y}\right)+\dot{w}_i\right] \tag{4}$$

Energy equation,

$$\frac{\partial h}{\partial t}+u\frac{\partial h}{\partial x}+v\frac{\partial h}{\partial y}=\frac{1}{\rho}\left[\frac{\partial}{\partial x}\left(\frac{\lambda_m}{C_{pm}}\frac{\partial h}{\partial x}\right)+\frac{\partial}{\partial y}\left(\frac{\lambda_m}{C_{pm}}\frac{\partial h}{\partial y}\right)\right] \tag{5}$$

where $\rho D_m=\lambda_m/C_{pm}$. The subscript m denotes the mixture and is omitted hereafter. The above dependent variables are related through the state equation,

$$p=\rho RT\sum_{i=1}^{N}(Y_i/W_i), \tag{6}$$

and the caloric equation of state

$$h_i=\int_{T_0}^{T}C_{pi}dT+\Delta H_i^0. \tag{7}$$

In this study, the fuel used is methane and the oxidizer is air. The chemical reaction expressing the combustion process is assumed to be a single-step, irreversible, finite-rate chemical reaction of methane and oxygen. The chemical reaction rate term $\dot{w}_i$ in Eq. (4) is evaluated from the following empirical formula proposed by Westbrook and Dryer[13] in terms of the molar concentration of methane per second:

$$k_{CH_4}=-A\exp(-E/RT)[CH_4]^a[O_2]^b, \tag{8}$$

where the pre-exponential factor A is $2.3\times10^7\ s^{-1}$, the activation energy $E=30.0$ kcal/mole, and the exponential factors a and b are -0.3 and 1.3, respectively. Equation (8) reproduces well the burning velocity estimated by a detailed reaction mechanism in the combustible range of mixture of methane and air[13].

3. Stretched Laminar Flamelet Model with Local Extinction

We investigate the edge flame structure based on the mixture fraction Z and the progress variable c. In this study, the mixture fraction is defined as the mass fraction of nitrogen. The progress variable is defined as

$$c=\frac{\phi}{\phi_0}, \tag{9}$$

which resembles, but is not identical to, the time-related variable proposed by Zhang et al.[5], who developed the transient flamelet model. Here, ϕ represents the integral value of the mass fraction of a major product Y_p in the mixture fraction space, say CO_2, and is defined by

$$\phi=\int_0^1 Y_p(Z,\chi_{st})\,dZ, \tag{10}$$

which represents the progress of the chemical reaction. Here, Y_p in mixture fraction space is dependent only on the mixture fraction and the stoichiometric scalar dissipation rate χ_{st} according to the flamelet concept[14),(15)], in which the stoichiometric scalar dissipation rate reflects the flame stretch effect. The notation ϕ_0 in Eq. (9) represents ϕ for the nonpremixed flame under the infinite reaction rate condition. Note that c is dependent on the stoichiometric scalar dissipation rate χ_{st}, and $c=0$ represents the unburned condition and $c=1$ represents burning under the infinite reaction rate condition. Hence by definition, the gradient vectors of c and Z are orthogonal and independent.

If we investigate the edge flame structure on the basis of the mixture fraction and the progress variable, we find that production and diffusion dominate the scalar structure, and that the scalar structure is dependent on the stoichiometric scalar dissipation rate.

The c transport equation is derived from the conservation equation of a product species and the transport equation of Z[5]. These equations are

$$\rho\frac{\partial Y_p}{\partial t}+\rho u_i\frac{\partial Y_p}{\partial x_i}=\rho D\frac{\partial^2 Y_p}{\partial x_i\partial x_i}+\dot{w}_p, \tag{11}$$

$$\rho\frac{\partial Z}{\partial t}+\rho u_i\frac{\partial Z}{\partial x_i}=\rho D\frac{\partial^2 Z}{\partial x_i\partial x_i}. \tag{12}$$

Here, we assume for simplicity that ρD is constant.

After rewriting the derivatives in Eq. (11) in consideration of Y_p as a function of c and Z, and then applying Eq. (12) to Eq. (11), the final form of the c equation becomes

$$\rho\frac{\partial c}{\partial t}+\rho u_i\frac{\partial c}{\partial x_i}-\rho D\frac{\partial^2 c}{\partial x_i\partial x_i}=\rho\dot{w}_c, \tag{13}$$

where $\dot{w}_c$ is

$$\rho\dot{w}_c=\frac{1}{\partial Y_p/\partial c}\left(\rho\frac{\chi_{ZZ}}{2}\cdot\frac{\partial^2 Y_p}{\partial Z^2}+\rho\frac{\chi_{cc}}{2}\cdot\frac{\partial^2 Y_p}{\partial c^2}+\rho\chi_{Zc}\cdot\frac{\partial^2 Y_p}{\partial Z\partial c}+\dot{w}_p\right), \tag{14}$$

and where

$$\chi_{ZZ}=2D\frac{\partial Z}{\partial x_i}\frac{\partial Z}{\partial x_i}, \tag{15}$$

$$\chi_{cc}=2D\frac{\partial c}{\partial x_i}\frac{\partial c}{\partial x_i}, \tag{16}$$

$$\chi_{Zc}=2D\frac{\partial Z}{\partial x_i}\frac{\partial c}{\partial x_i}. \tag{17}$$

The scalar dissipation rate χ_{zz} represents the dissipation rate of Z, χ_{cc} represents the dissipation rate of c, and χ_{zc} represents the dissipation rate of both Z and c.

We can now investigate the edge flame structure in detail in the frame of Z and c. The governing equations are transformed to the $Z-c$ coordinate system by the following transformations:

$$\frac{\partial}{\partial t}=\frac{\partial}{\partial\tau}+\frac{\partial}{\partial Z}\frac{\partial Z}{\partial t}+\frac{\partial}{\partial c}\frac{\partial c}{\partial t}, \tag{18}$$

and

$$\frac{\partial}{\partial x_i}=\frac{\partial}{\partial Z}\frac{\partial Z}{\partial x_i}+\frac{\partial}{\partial c}\frac{\partial c}{\partial x_i}, \tag{19}$$

where $\tau=t$. The energy balance equation in terms of temperature T given by

$$\rho\frac{\partial T}{\partial t}+\rho u_i\frac{\partial T}{\partial x_i}=\rho D\frac{\partial^2 T}{\partial x_i\partial x_i}+\left(\frac{-\Delta h}{C_p}\right)\dot{w}_f \tag{20}$$

is written in the frame of Z and c as

$$\rho\frac{\partial T}{\partial\tau}=\rho\frac{\chi_{ZZ}}{2}\frac{\partial^2 T}{\partial Z^2}+\rho\frac{\chi_{cc}}{2}\frac{\partial^2 T}{\partial c^2}+\rho\chi_{Zc}\frac{\partial^2 T}{\partial Z\partial c}-\rho\frac{\partial T}{\partial c}\dot{w}_c+\left(\frac{-\Delta h}{C_p}\right)\dot{w}_f. \tag{21}$$

Here, the subscript f stands for the fuel. In addition to the above assumptions, the specific heat at constant pressure C_p is assumed to be constant and the enthalpy flux term is neglected as smaller than the error introduced by assuming the constant C_p. The pressure variation is also neglected. Equations (12) and (13) are used for the derivation of Eq. (21). Note that Eq. (21) does not include convection terms for the advection of Z and c. The term on the left-hand side represents temporal change, and the first three terms on the right are thermal diffusion terms with respect to Z, c, and both Z and c. The fourth and fifth terms are the source terms for c and heat. Here, careful consideration is required regarding the interpretation of the source term for c. For simplicity, let us consider a steady state problem so as to ignore the left-hand term. A positive value of $\dot{w}_c$ implies that c will increase if the temperature remains constant, with the net effect that temperature is reduced. For the purpose of the discussion, each term is enumerated first to sixth from the left-hand side.

4. Geometry and Boundary Conditions

We consider semi-planar steady-state flames oriented normal to the x-direction with air flow into the calculation domain at $x=0$ and fuel introduced at $x=10$ mm. Calculations were performed for half the two-dimensional flow field assuming symmetrical geometry, as shown in Fig. 1. The computational domain extends to 20 mm in the y-direction. Although steady-state solutions are sought, the time-derivative terms are retained in the governing equations because the numerical algorithm adopted is based on the time-dependent SIMPLE approach[16]. The governing equations are discretized by the control volume approach with accuracies of temporally $O(\Delta t)$ and spatially $O(\Delta x^2, \Delta y^2)$. The present SIMPLE method is as follows: (1) Guess pressure p^*, (2) Solve momentum equations to get u^* and v^*, which are imperfect velocity fields based on the guessed pressure field p^*, (3) Calculate the source term b for pressure correction p' equation. If $b=0$, STOP, (4) Solve p' equation, and calculate velocity corrections u' and v', (5) Update velocities using $u=u^*+u'$ and $v=v^*+v'$, (6) Solve continuity equations of species and energy equation, and (7) Return to (2) with p^* replaced by p. The present convergent constraint is 1×10^{-5} in terms of relative error. The solution of the problem requires that appropriate boundary conditions be imposed. The inlet x-velocities u are specified in Table 1 for the three calculation cases. The y-velocity component v is zero at each inlet. The derivatives of other dependent variables with re-

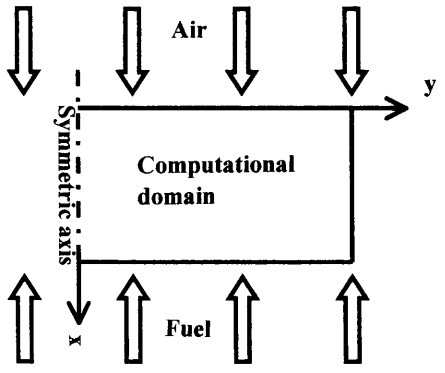

Fig. 1 Computational domain and coordinate system for two-dimensional counterflow field

Table 1 Calculation conditions

	Inflow velocity
case1	0≦y≦8(mm) : 5(cm/s) 8<y≦11 : 25 11<y≦20 : 5
case2	0≦y≦5 : 25 5<y≦20 : 5
case3	0≦y≦3 : 20 3<y≦20 : 5

spect to x are set as zeroes at each inlet. At the symmetric boundary ($y=0$), we set $v=0$ and the y-derivatives of other dependent variables as zeroes. The outlet is dealt with as a free flow-out boundary; the y-derivatives of the u-velocity component, the mass fractions of species, and the temperature are zeroes, and the v-velocity component is determined by the continuity equation. The SIMPLE algorithm requires boundary conditions for the pressure correction equation. The inlet and symmetry boundaries, however, no longer require boundary conditions because the velocity boundary conditions are already specified, and the pressure difference to be corrected is set at zero at the outlet[16]. The supply temperature is 298 K, and a grid of 100 points in the x-direction (the step size $\Delta x = 0.1$ mm) and 150 points in the y-direction ($\Delta y = 0.16$ mm) is imposed for each calculation. Time step is 5×10^{-6} s. Thermophysical and chemical data are taken from the CHEMKIN software package[17),(18)]. Calculations were primarily performed for the three cases in Table 1, where flames are categorized into two quenching patterns; extinction downstream and extinction upstream of the flame. Case 1 corresponds to downstream extinction, for which the inflow condition is given by a high inflow velocity of 25 cm/s between $y=8$ mm and 11 mm, while the remainder is 5 cm/s. Cases 2 and 3 are examples of upstream extinction. In case 2, the reactants flow into the calculation domain at a velocity of 25 cm/s at the center between $y=0$ and 5 mm, while the remaining area has a lower velocity of 5 cm/s. In case 3, the higher velocity is changed to 20 cm/s, applied to the interval between $y=0$ and 3 mm. Other extra calculations were performed in order to obtain the flame structure of a fully burning counterflow nonpremixed flame without local extinction. The scalar dissipation rate at the extinction of the uniform counterflow nonpremixed flame was $1.8\,s^{-1}$. This value is much lower than the $7.8\,s^{-1}$ estimated by Peters[14] on the basis of an experimental result of Tsuji and Yamaoka[19], and is thought to depend strongly on the reaction rate expression used here. As mentioned above, Eq. (8) can reproduce the burning velocity. This means that source terms in the species conservation equations are adequately represented in the frame of the one-step, irreversible, finite-rate reaction and can well reproduce the scalar field regardless of combustion types. The underestimation of the quenching scalar dissipation rate must be caused by intermediate reactions, as reported by Takahashi et al.[20] and Takahashi and Katta[21]. Accordingly, we used the rate formula given by Eq. (8) without modification because any modification would damage the validity of the results.

5. Results and Discussion

Figure 2 shows the calculated flow field and the scalar field related to temperature, heat-release rate, mixture fraction, and the progress variable for a steady, locally quenching, counterflow nonpremixed flame for case 1. The temperature, scalar dissipation rate, and progress variable profiles on the stoichiometric line are shown in Fig. 3. The stoichiometric mixture fraction of the present fuel Z_{st} is 0.054 8. Figures 4 and 5 show the results for case 2, in which the flame is not steady, moving very slowly in the y-direction. Each flame is quenched locally near the position where the fuel and air collide at high inflow velocity, corresponding to a region of higher scalar dissipation rate. A key point is that the flames always extinguish at below the extinction value of the scalar dissipation rate required for spatially uniform stretch. This result is in accordance with the experimental finding of Shay and Ronney[22], and is attributable to the decrease in the extinction Damköhler number at the flame edge, in comparison to a uniformly strained flame, as predicted by Buckmaster and Weber[2]. On the basis of the prediction, the ratio of the strain rate at the steady flame edge to the extinction strain rate of a uniformly strained flame is estimated to be 0.75 for the present cases. Moreover, we notice in Figs. 3 (II) and 5 (II) that the scalar dissipation rate increases slightly immediately ahead of the point at which the flame temperature starts to decrease. This position corresponds to the point at which the diffusion coefficient D increases rapidly due to the rise in temperature in the direction of the flame. The mixture fraction gradient $\partial Z/\partial x$ along the stoichiometric line relaxes gradually (not shown). Therefore, this phenomenon, which is determined by the product of the diffusion coefficient and the square of the mixture fraction gradient $2D(\partial Z/\partial x_i)^2$, is caused by rapid reaction. Moving away from the flame, the temperature initially decreases rapidly, followed by a 5 to 12-mm preheat region with a relatively gradual decrease in temperature. The maximum temperature ridgelines tend to deviate from the stoichiometric lines indicated by the Z_{st} lines in Figs. 2 (II) and 4 (II). The progress variable c decreases somewhat slower than the temperature. The heat-release rates in cases 1 and 2 shown in Figs. 2 (III) and 4 (III) have hook-shaped distributions, with the tip directed towards the fuel-lean side (air side). Takahashi et al.[20] reported similar distributions in the heat-release rate at the flame base of jet diffusion flames, the peak spot termed the reaction kernel, by implementing calculations of co-flow methane-air jet

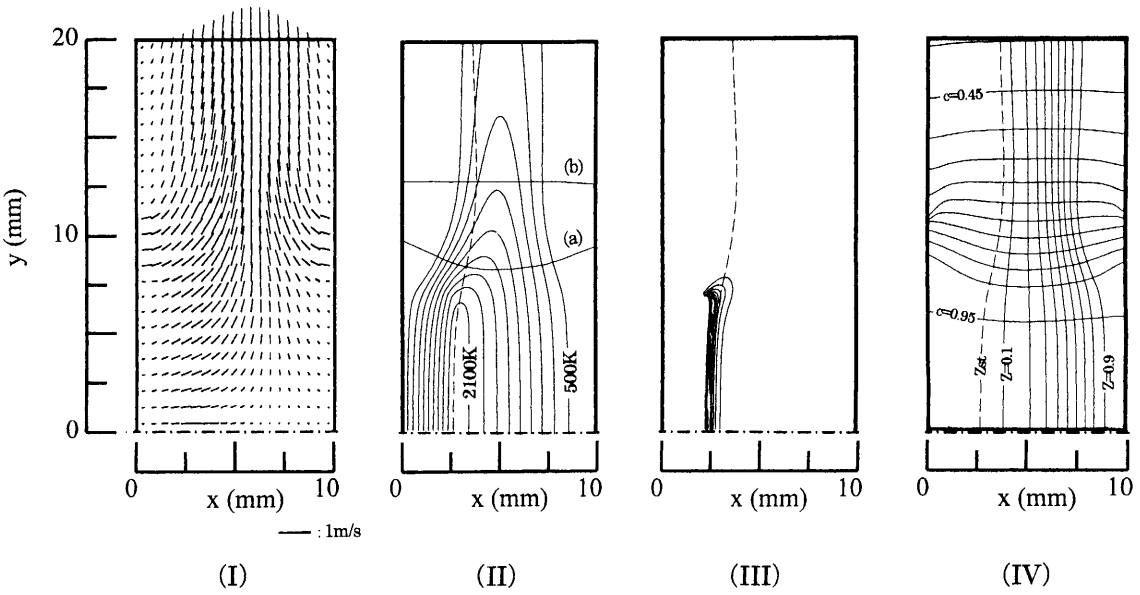

Fig. 2 Calculated flow and scalar fields for case 1: (I) Velocity vectors, (II) temperature, (III) heat-release rate (30 – 300 MJ/m^{3}s), and (IV) distribution of mixture fraction and progress variable

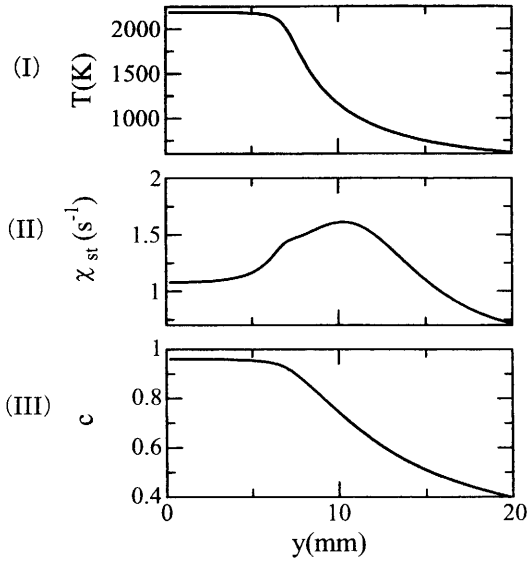

Fig. 3 (I) Temperature, (II) scalar dissipation rate, and (III) progress variable for stoichiometric line of case 1

diffusion flames with a detailed chemistry model. In their study, it was concluded that radicals diffusing radially near the reaction kernel cause the expansion of the flame base towards the fuel-lean side. Our results show very similar flame edges despite the fact that the calculations are based on a simple one-step reaction. Moreover, the heat-release rate distributions maintain a consistent shape regardless of the direction of flow against the flame edge, as shown in Figs. 2 (III) and 4 (III). This implies that the effect of partial premixing is negligible in our calculation; the mixing time is too short to lead to triple flame[23]. In our geometry, temperature gradients are steeper on the air side than on the fuel side, as shown in Figs. 2 (II) and 4 (II). This is expected to enhance the diffusion of scalars on the air side, expanding the flame edge in that direction. Consequently, the shape of the edge flame is closely related to the diffusion process.

Takahashi and Katta[21] also investigated the effect of the one-step global chemistry on numerical results in the jet diffusion flames and reported a heat release-rate distribution hooked on the rich side different from the results by the detailed chemistry model and also the present results. However, this result is strongly affected by a rate equation used in their study which overestimates on the rich side than the present one, and does not reflect the scalar field to be evaluated.

Figure 6 shows the progress variable for each case as a function of the scalar dissipation rate, which is dependent on the stoichiometry. Each c-χ_{st} curve can be divided into three regions. The first is the upper c region, having a negative slope with respect to χ_{st} and corresponding to the fully burning flame condition dominated by the reaction and diffusion with respect to Z. The next corresponds to the mid c region and is characterized by a more rapid decrease in c. The reaction is dramatically weakened in this region, but not zero. In the lower c region, the decrease in c is slower again, and the reaction does not proceed. This region corresponds to the preheat region. The finite value of c is attributable to the diffusion of products from the flame. Two conditions, indicated by the crossing points in the figure, will be used in the following discussion to compare the flame structures. The crossing point of case 1 and case 2 corresponds to cross-section (a) in Fig. 2 and cross-section (c) in Fig. 4 under the condition that $\chi_{st} = 1.52\,s^{-1}$

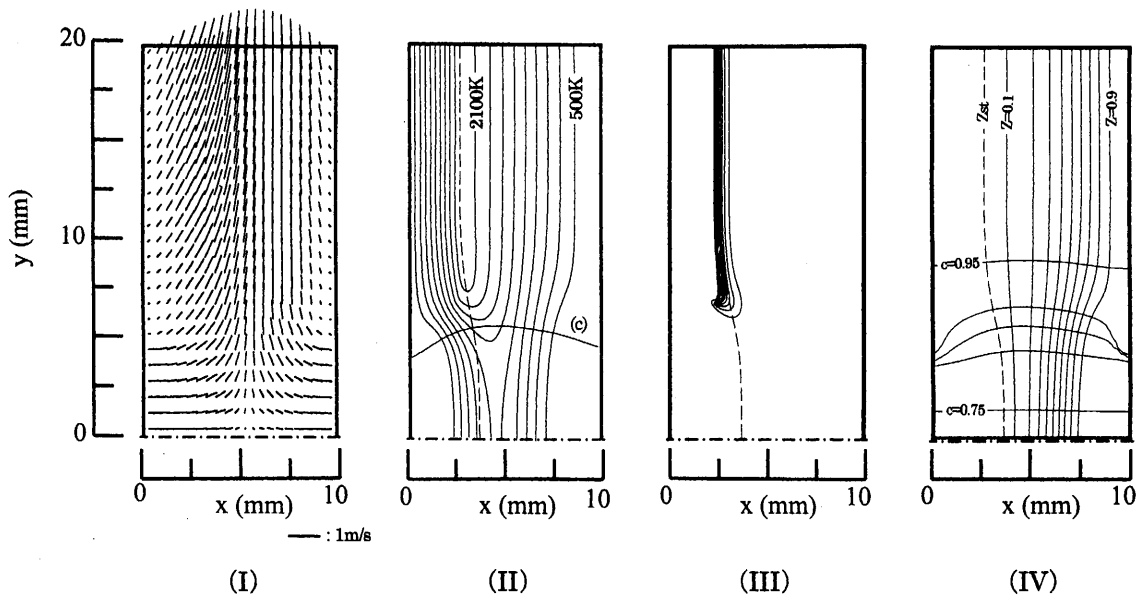

Fig. 4 Calculated flow and scalar fields for case 2: (I) Velocity vectors, (II) temperature, (III) heat-release rate (30 – 300 MJ/m^3 s), and (IV) distribution of mixture fraction and progress variable

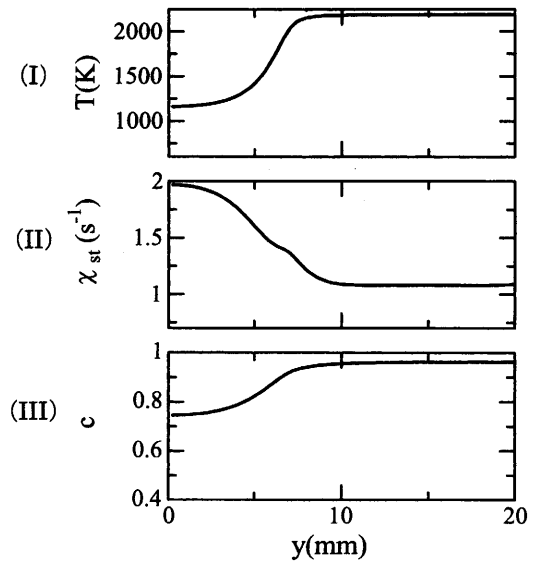

Fig. 5 (I) Temperature, (II) scalar dissipation rate, and (III) progress variable for stoichiometric line of case 2

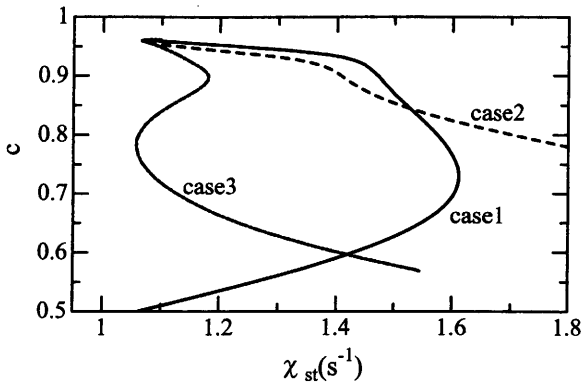

Fig. 6 Progress variable for each case as a function of scalar dissipation rate

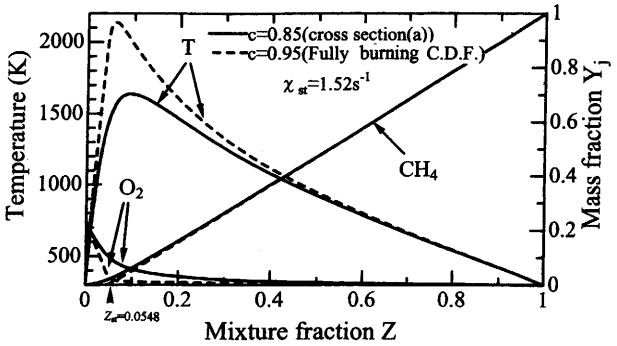

Fig. 7 Comparison of flame structures between fully burning counterflow nonpremixed flame without extinction and cross-section (a) of case 1 (Fig. 2) for the same scalar dissipation rate (χ_{st} = 1.52 s^{-1}). CDF: counterflow diffusion flame (nonpremixed)

and $c = 0.85$. The crossing point of case 1 and case 3 corresponds to cross-section (b) in Fig. 2 and cross-section (d) (not shown) under the condition that $\chi_{st} = 1.42\ s^{-1}$ and $c = 0.59$.

Figure 7 shows a comparison of flame structures between a fully burning counterflow nonpremixed flame without extinction and a flame of cross-section (a), for a given scalar dissipation rate of $\chi_{st} = 1.52\ s^{-1}$ and dissimilar progress variables $c = 0.95$ and 0.85, respectively. The flame structures differ even though the scalar dissipation rates are matched. For case 1, the flame temperature decreases at close to stoichiometry, and the leakage of fuel and oxidizer increases across the reaction region due to the decay in the reaction rate. This implies that the mix-

ture fraction and scalar dissipation rate at the edge of nonpremixed flames with local extinction are not the sole factors affecting the flame structure.

We then investigated the balance of heat transfer on the basis of Eq. (21) in order to clarify the important factors that affect the flame structure. Figure 8 shows the heat transfer balances of the fully burning counterflow nonpremixed flame without local extinction and for cross-section (a) of case 1. Here, the terms are numbered in reference to the order in Eq. (21). A minor unbalance of heat transfer noticed in Fig. 8 (II) comes from the approximations in Eq. (21). For the fully burning counterflow nonpremixed flame, the heat source term (term 6) balances the Z-directional heat diffusion term (term 2). This implies that the flame structure is dependent on the mixture fraction and scalar dissipation rate involved in the diffusion term (term 2). For cross-section (a) of case 1, an additional term becomes important. The term is the production term for c (term 5). Here, term 5 is also attributed to the Z-directional diffusion of the product corresponding to the first term on the right-hand side of Eq. (14), being the contribution of other smaller terms on the cross-section (not shown). As the calculated Z-directional diffusion term of the product is negative, the production rate $\dot{w}_c$ is also negative. As mentioned above, the negative value of $\dot{w}_c$ represents the production of thermal energy. We can conclude from Fig. 8 (II) that terms 2 and 5 are dominant for the conditions of cross-section (a), and the effect of the heat source term (term 6) is weakened. This implies that the edge flame structure is governed in part by the property represented by the progress variable.

Lastly, we investigated the above two cases under the condition of identical scalar dissipation rate and progress variable. The first case examined was that for $\chi_{st} = 1.52\,s^{-1}$ and $c = 0.85$, corresponding to cross-sections (a) and (c) of cases 1 and 2 (Figs. 2 and 4). A comparison of the flame structures is shown in Fig. 9; the flame structures are almost coincident. The case for $\chi_{st} = 1.42\,s^{-1}$ and $c = 0.59$ is shown in Fig. 10, corresponding to cross-sections (b) and (d) of cases 1 and 3. This condition involves the preheat region. The heat transfer balances are also compared in the figure, with the above- mentioned minor unbalance. The flame structures (Fig. 10 (I)) are roughly coincident, although there is a minor dissimilarity on the fuel-lean side. The flame structure in this region is also dominated by terms 2 and 5, as shown in Fig. 10 (II) and (III). The small deviation is due to the expansion of the flame base towards the fuel-lean side with a steeper temperature gradient, as mentioned above. In the nonreaction preheat region, the stoichiometric scalar dissipation rate is not a factor in the scalar structure in the mixture fraction space. For the fully burning flame, χ_{st} is important because term 2 becomes significant only in regions approaching stoichiometry, as shown in Fig. 8 (I). In the preheat region, as a number of scalars including temperature are transferred from the first two regions, diffusion processes around stoichiometry dominate the scalar structure. These results indicate that three parameters; the mixture fraction, the scalar dissipation rate, and the progress variable, are the primary factors that affect the edge flame structure of nonpremixed flames with local extinction.

These findings are closely tied with the single-step, irreversible, finite-rate reaction model employed in this

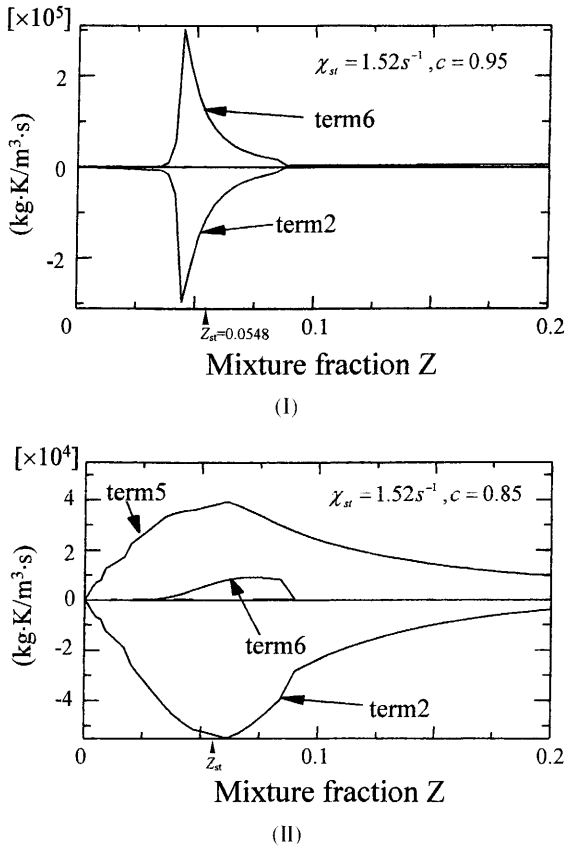

Fig. 8 Heat transfer balances: (I) Fully burning counterflow nonpremixed flame without extinction, and (II) cross-section (a) of case 1 (Fig. 2)

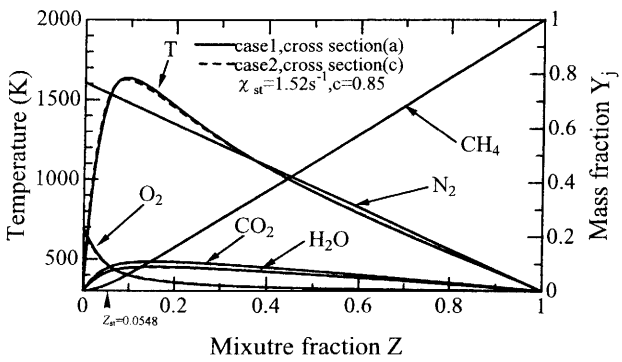

Fig. 9 Comparison of flame structures between cross-section (a) of case 1 and cross-section (c) of case 2 for the condition of $\chi_{st} = 1.52\,s^{-1}$ and $c = 0.85$

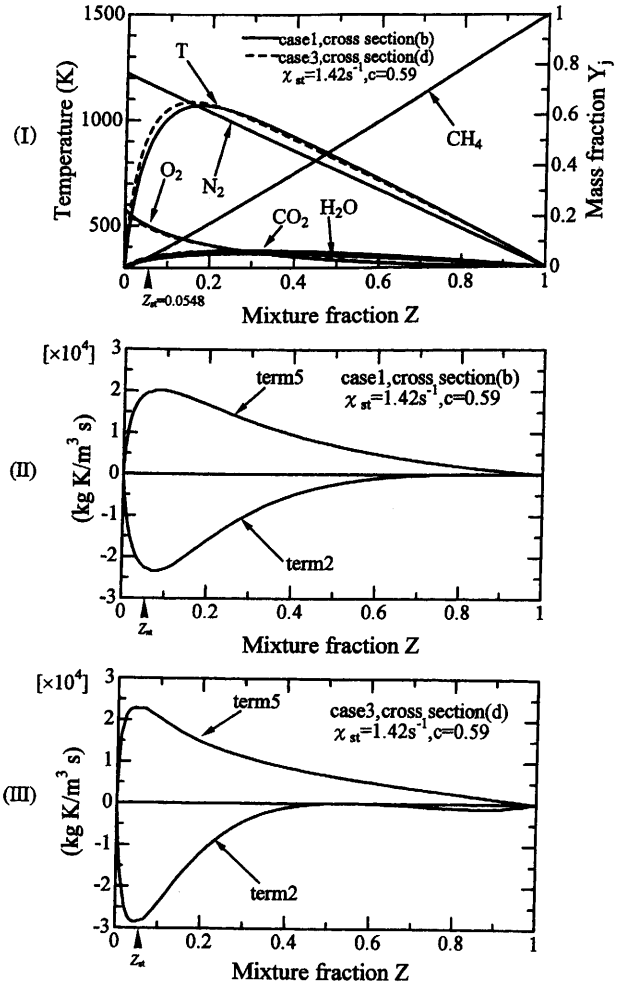

Fig. 10 (I) Comparison of flame structures between cross-section (b) of case 1 (Fig. 2) and cross-section (d) of case 3 (not shown). (II) Heat transfer balance for cross-section (b). (III) Heat transfer balance for cross-section (d). Conditions are $\chi_{st} = 1.42\,s^{-1}$ and $c = 0.59$.

study. Investigations using a detailed chemical-kinetic model will be pursued in future studies.

6. Conclusion

The edge flame structure of counterflow nonpremixed flames with local extinction was numerically investigated in the two-dimensional counterflow configuration with step-like inflows. The flame structure was discussed based on the mixture fraction and a newly defined progress variable derived from the transient flamelet concept. This system has not been discussed explicitly to date. The progress variable is defined as the normalized integral of the mass fraction of a product in the mixture fraction space, and the reference value is based on a nonpremixed flame with infinite reaction rate. The edge flame structure was classified into three categories fully burning flame, in which the heat transfer is balanced between Z-direction diffusion and the source; weakened flame, for which the reaction is very weak; and a preheat region, where the reaction ceases. Each type of flame structure was well characterized by the mixture fraction, the scalar dissipation rate, and the progress variable, with only a minor discrepancy for the preheat region. The discrepancy is attributed to the fact that the stoichiometric scalar dissipation rate is not a factor affecting the scalar structure in the non-reaction region. However, in the preheat region, as a number of scalars including temperature are transferred from the reaction region of the first two regions, the diffusion processes around stoichiometry continue to dominate the scalar structure. These three parameters are considered to be important factors affecting the edge flame structure of nonpremixed flames with local extinction.

The authors express their gratitude to Y. Onuma and K. Yamamoto for valuable comments.

References

(1) Idera, M., Motoyasu, A., Morikawa, M., Noda, S. and Onuma, Y., NOx Formation in Lifted Nonpremixed Jet Flames, 37th Japanese Symp. on Combust., (in Japanese), (1999), pp.113–114.

(2) Buckmaster, J. and Weber, R., Edge-Flame-Holding, Proc. Combustion Institute, Vol.26 (1996), pp.1143–1149.

(3) Buckmaster, J., Edge-Flames and Their Stability, Combust. Sci. Tech., Vol.115 (1996), pp.41–63.

(4) Buckmaster, J., Edge-Flames, J. Eng. Math., Vol.31 (1997), pp.269–284.

(5) Zhang, Y., Rogg, B. and Bray, K.N.C., 2-D Simulation of Turbulent Autoignition with Transient Laminar Flamelet Source Term Closure, Combust. Sci. Tech., Vol.105 (1995), pp.211–227.

(6) Mastorakos, E., Baritaud, T.A. and Poinsot, T.J., Numerical Simulations of Autoignition in Turbulent Mixing Flows, Combust. Flame, Vol.109 (1997), pp.198–223.

(7) Müller, C.M., Breitbach, H. and Peters, N., Partially Premixed Turbulent Flame Propagation in Jet Flames, Proc. Combustion Institute, Vol.25 (1994), pp.1099–1106.

(8) Buckmaster, J. and Matalon, M., Anomalous Lewis Number Effects in Tribrachial Flames, Proc. Combustion Institute, Vol.22 (1988), pp.1527–1535.

(9) Dold, J.W., Flame Propagation in a Nonuniform Mixture: Analysis of a Slowly Varying Triple Flame, Combust. Flame, Vol.76 (1989), pp.71–88.

(10) Kioni, P.N., Rogg, B., Bray, K.N.C. and Liñán, A., Flame Spread in Laminar Mixing Layers: The Triple Flame, Combust. Flame, Vol.95 (1993), pp.276–290.

(11) Kioni, P.N., Bray, K.N.C., Greenhalgh, D.A. and Rogg, B., Experimental and Numerical Studies of a Triple Flame, Combust. Flame, Vol.116 (1999), pp.192–206.

(12) Ruetsch, G.R., Vervisch, L. and Liñán, A., Effects of Heat Release on Triple Flames, Phys. Fluids, Vol.7, No.6 (1995), pp.1447–1454.

(13) Westbrook, C.K. and Dryer, F.L., Simplified Reaction Mechanisms for the Oxidation of Hydrocarbon Fuels in

Flames, Combust. Sci. Tech., Vol.27 (1981), pp.31–43.
(14) Peters, N., Local Quenching Due to Flame Stretch and Non-Premixed Turbulent Combustion, Combust. Sci. Tech., Vol.30 (1983), pp.1–17.
(15) Peters, N., Laminar Diffusion Flamelet Models in Non-Premixed Turbulent Combustion, Prog. Energy Combust. Sci., Vol.10 (1984), pp.319–339.
(16) Patankar, S.V., Numerical Heat Transfer and Fluid Flow, (1980), Hemisphere Publishing Corporation.
(17) Kee, R.J., Dixion-Lewis, G., Warnatz, J., Coltrin, M.E. and Miller, J.A., A Fortran Computer Code Package for the Evaluation of Gas-Phase, Multicomponent Transport Properties, Sandia Report, SAND86-8246, (1986).
(18) Kee, R.J., Rupley, F.M. and Miller, J.A., Chemkin-II: A Fortran Chemical Kinetics Package for the Analysis of Gas Phase Chemical Kinetics, Sandia Report, SAND89-8009B, (1989).
(19) Tsuji, H. and Yamaoka, I., The Structure of Counterflow Diffusion Flames in the Forward Stagnation Region of a Porous Cylinder, Proc. Combustion Institute, Vol.12 (1969), pp.997–1005.
(20) Takahashi, F., Schmoll, W.J. and Katta, V.R., Attachment Mechanisms of Diffusion Flames, Proc. Combustion Institute, Vol.27 (1998), pp.675–684.
(21) Takahashi, F. and Katta, V.R., A Reaction Kernel Hypothesis for the Stability Limit of Methane Jet Diffusion Flames, Proc. Combustion Institute, Vol.28 (2000), pp.2071–2078.
(22) Shay, M.L. and Ronney, P.D., Nonpremixed Edge Flames in Spatially Varying Straining Flows, Combust. Flame, Vol.112 (1998), pp.171–180.
(23) Chung, S.H. and Lee, B.J., On the Characteristics of Laminar Lifted Flames in a Nonpremixed Jet, Combust. Flame, Vol.86 (1991), pp.62–72.